20th International Congress on Sound & Vibration

ICSV20
Bangkok,Thailand
7-11 July 2013

SKEW-CIRCULANT MATRIX FORMULATION FOR TRANSIENT NEAR-FIELD ACOUSTICAL HOLOGRAPHY

Jean Michel Attendu and Annie Ross

CREPEC, Department of Mechanical Engineering, École Polytechnique de Montréal, CP 6079 station Centre-ville, Montréal (Québec), Canada, H3C 3A7

e-mail: annie.ross@polymtl.ca

Near-field acoustical holography is a widely used technique to visualize sound in three dimensions. However, the monitoring of short transients with such method is inaccurate because of the generation of wraparound. This is due to solving discrete convolutions with the fast Fourier transform algorithm. Yet, visualization of transient signals leads to useful applications, such as investigation of impact noises in industrial environments, which is a significant cause of hearing impairment. Typical solution to this problem involves adding zero padding to avoid wraparound; however, calculations are thus increased substantially. In the present paper, a solution is proposed based on the use of circulant and skew-circulant matrices. The method allows resolution of the discrete convolution with the fast Fourier transform algorithm without generating wraparound error. The resulting convolution is linear and does not require the use of zero padding. Current development of the method allows its application over the time domain, and standard convolution is applied to the spatial domains. When fully developed in three dimensions, computation cost should be similar to that of the classical formulation without zero padding. In this paper, the theoretical development of the circulant matrix holography method in 1D is presented, followed by an application to simulated data. The resulting sound field is then compared to the field obtained with standard near-field acoustical holography. It is shown that the proposed method is an efficient solution to accurately monitor transient sounds without generating wraparound error.

1. Introduction

Near-field acoustical holography (NAH) was established as a proficient method to visualize stationary acoustic fields [1-3]. Propagation of a measured sound pressure field is performed through convolution with a Green's function. To avoid lengthy convolution in the time and space domains, the method is typically applied using the convolution property of the Fourier transform. For finite signals, the corresponding convolution is circular, which is adequate in the case of periodic signals. However for non-periodic signals, wraparound error is generated in the process. Such error is usually suppressed by adding zero padding beyond the boundaries of the signal, resulting in increased computing requirements.

Solutions were proposed to overcome these problems, by solving the convolution product in time and space domains [4-5] or by applying a Laplace transform to decrease the effect of wraparound [6]. However, these methods either lead to heavy computing requirements or do not suppress wrapa-

round entirely. As a more promising solution, a novel adaptation of NAH was developed. The proposed solution relies on the use of circulant matrices to perform linear convolution. The properties of these matrices allow using Fourier transforms. This approach successfully suppresses wraparound error and is compatible with the use of the fast Fourier transform (FFT), thus keeping a lighter load of computational operations. In this paper, mathematical description of this novel approach is presented. It is followed by a detailed description of the wraparound error phenomenon. Finally, the effectiveness of the proposed method is investigated with short-time radiation of a baffled piston excited with a Gaussian pulsed velocity for both standard NAH and circulant NAH methods.

2. Circulant matrix based NAH

The novel formulation for circulant matrix based NAH is developed in order to suppress wraparound error both in the time and space domains. Linear convolution is obtained from the sum of circulant and skew-circulant matrices. These matrices can be diagonalized by a discrete Fourier transform, and are contained in a linear equation that can be solved using fast Fourier transform.

2.1 Circular and linear convolution using circulant matrices

Circulant matrices [7] are Toeplitz matrices for which the elements of each row are identical to those of the previous row, but are moved one position to the right and wrapped around. Thus, the N by N square matrix is defined by the values of its first row. For vector $p = [p_1\ p_2\ p_3\ \dots\ p_N]$, the corresponding circulant matrix P is represented as:

$$P = \begin{bmatrix} p_1 & p_2 & p_3 & \cdots & p_N \\ p_N & p_1 & p_2 & & p_{N-1} \\ & \vdots & & \ddots & \vdots \\ p_2 & p_3 & p_4 & \cdots & p_1 \end{bmatrix} \tag{1}$$

A skew-circulant matrix is similar to circulant, except the sign of all elements under the main diagonal is changed. Skew-circulants are also known as negacylic matrices. N by N skew-circulant for vector p is given by:

$$Q = \begin{bmatrix} p_1 & p_2 & p_3 & \cdots & p_N \\ -p_N & p_1 & p_2 & & p_{N-1} \\ & \vdots & & \ddots & \vdots \\ -p_2 & -p_3 & -p_4 & \cdots & p_1 \end{bmatrix} \tag{2}$$

Circulants can be used to express discrete convolution products for finite vectors. Since analytical convolution is defined over an infinite domain, it is required to make some assumptions in order to convolve finite signals. Two types of discrete convolutions are defined. First, in circular convolution, it is supposed that the finite signals are repeated periodically over an infinite extent. Mathematically, the circular convolution of vectors p and g, both of length N, can be expressed as [8]:

$$(p * g)(n) \equiv \sum_{m=0}^{N-1} \left(\sum_{k=-\infty}^{\infty} p[m + kN] \right) g_N[n - m] \tag{3}$$

This results in a periodical pattern of length N. The pattern for $(p * g)$ can be obtained by performing a matrix product of matrix P and vector g, where T denotes the transpose:

$$(p * g)(n) = \begin{bmatrix} p_1 & p_2 & p_3 & \cdots & p_N \\ p_N & p_1 & p_2 & & p_{N-1} \\ & \vdots & & \ddots & \vdots \\ p_2 & p_3 & p_4 & \cdots & p_1 \end{bmatrix}^T \begin{bmatrix} g_1 \\ g_2 \\ \vdots \\ g_N \end{bmatrix} \tag{4}$$

The second type of discrete convolution is the linear convolution, for which it is assumed that all values outside the range of definition of the vectors are null. The convolved vectors of length *N* result in a sequence of *2N-1* points, and values outside this range are zero. The linear convolution is expressed as the following, for $k = \{0, 1, 2, \ldots, 2N-1\}$ [8]:

$$(p * g)(n) = \sum_{m=0}^{n} p(n-m)g(m) \tag{5}$$

In this case, it is also possible to express the convolution as a matrix multiplication:

$$(p * g)(n) = \left(\begin{bmatrix} p_1 & 0 & 0 & \cdots & 0 \\ p_N & p_1 & 0 & & 0 \\ & \vdots & & \ddots & \vdots \\ p_2 & p_3 & p_4 & \cdots & p_1 \end{bmatrix} \middle| \begin{bmatrix} 0 & p_2 & p_3 & \cdots & p_N \\ 0 & 0 & p_2 & & p_{N-1} \\ & \vdots & & \ddots & \vdots \\ 0 & 0 & 0 & \cdots & 0 \end{bmatrix} \right) \begin{bmatrix} g_1 \\ g_2 \\ \vdots \\ g_N \end{bmatrix} \tag{6}$$

The augmented matrix is composed of the upper and lower triangular Toeplitz matrices which, merged together, form the matrix *P*. Lower and upper parts are referred as *L* and *U* respectively (which should not be confused with *LU* factorisation). Multiplication should be done independently for each part of the *LU* matrix. Resulting vectors should be merged, ignoring the last value of the $U \cdot g$ product (which is zero), ensuing a vector of length *2N-1*.

Circular and linear convolutions are illustrated in Fig. 1 for vectors *f* and *g* of length *N*=4. Fig. 1a) and 1b) illustrate signals to be convolved. In Fig. 1c), circular convolution is shown; it is noted that the length of the vector is the same as the length of the input signals. If the periodical assumption for *f(x)* and *g(x)* is incorrect, $(f*g)_{circ}$ includes wraparound error. In Fig. d), linear convolution is presented; the length of the vector is *2N-1*. Linear convolution can also be obtained by performing a circular convolution on a zero-padded signal.

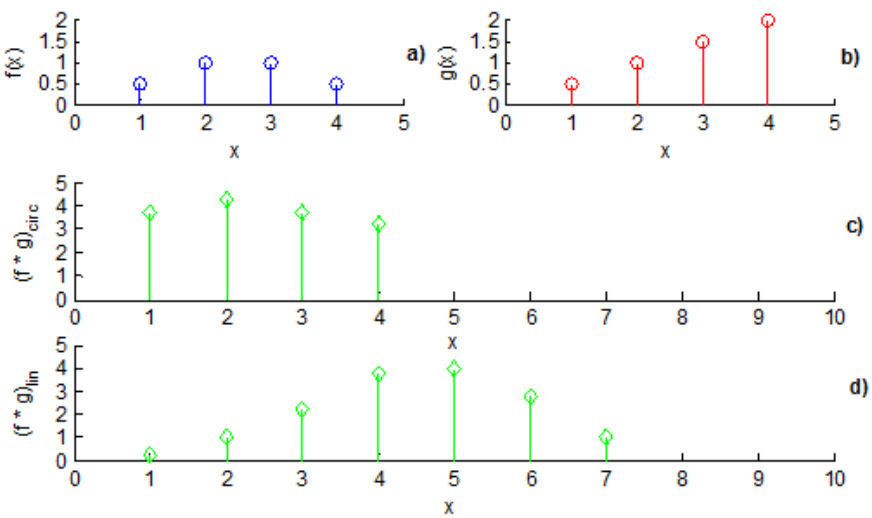

Fig.1 Comparison between circular and linear convolutions

2.2 Basic formulation of circulant NAH

The goal of circulant NAH is to express the discrete convolution of the pressure field and the Green's function as a linear convolution instead of a circular convolution without increasing the size of the input data. Also, it is intended to perform the linear convolution using the convolution property of the Fourier transform in order to benefit from the computing speed of the fast Fourier transform (FFT) algorithm.

This can be achieved by expressing the lower and upper triangular parts of P as the average of the circulant matrix P and its skew-circulant form Q. This is shown for matrix L:

$$\begin{aligned} L \cdot g &= \begin{bmatrix} p_1 & p_2 & p_3 & \cdots & p_N \\ 0 & p_1 & p_2 & & p_{N-1} \\ & \vdots & & \ddots & \vdots \\ 0 & 0 & 0 & \cdots & p_1 \end{bmatrix}^T \begin{bmatrix} g_1 \\ g_2 \\ \vdots \\ g_N \end{bmatrix} \\ &= \frac{1}{2}\left(\begin{bmatrix} p_1 & p_2 & p_3 & \cdots & p_N \\ p_N & p_1 & p_2 & & p_{N-1} \\ & \vdots & & \ddots & \vdots \\ p_2 & p_3 & p_4 & \cdots & p_1 \end{bmatrix} + \begin{bmatrix} p_1 & p_2 & p_3 & \cdots & p_N \\ -p_N & p_1 & p_2 & & p_{N-1} \\ & \vdots & & \ddots & \vdots \\ -p_2 & -p_3 & -p_4 & \cdots & p_1 \end{bmatrix} \right)^T \begin{bmatrix} g_1 \\ g_2 \\ \vdots \\ g_N \end{bmatrix} \end{aligned} \tag{7}$$

For matrix U, skew-circulant matrix is subtracted from the circulant. The eigenvectors of circulants are linearly independent [8] and thus, from the matrix theory, circulants can be diagonalized in accordance to their eigenvalue equation:

$$FP = \Lambda \mathrm{F} \tag{8}$$

where F is the matrix composed of all eigenvectors of P and Λ is a diagonal matrix containing the eigenvalues of P. For circulants, it turns out that F is in fact the inverse discrete Fourier transform (DFT^{-1}) operator in its matrix form. In other words, F is a matrix that, when multiplied to a given vector, results in the inverse DFT of the vector [7]:

$$F = \frac{1}{\sqrt{N}} \begin{bmatrix} \omega^0 & \omega^0 & \omega^0 & & \omega^0 \\ \omega^0 & \omega^1 & \omega^2 & \cdots & \omega^{(N-1)} \\ \omega^0 & \omega^2 & \omega^4 & & \omega^{2(N-1)} \\ & \vdots & & \ddots & \vdots \\ \omega^0 & \omega^{N-1} & \omega^{2(N-1)} & \cdots & \omega^{(N-1)(N-1)} \end{bmatrix} \tag{9}$$

with

$$\omega = e^{\frac{2\pi i}{N}} \tag{10}$$

Following this definition, it is noted that the inverse of F also is its complex conjugate $F^{-1} = F^*$. The eigenvalue matrix Λ is defined as:

$$\Lambda(k) = \begin{bmatrix} \lambda(1) & 0 & 0 & \dots & 0 \\ 0 & \lambda(2) & 0 & \dots & 0 \\ 0 & 0 & \lambda(3) & \dots & 0 \\ \vdots & \vdots & \vdots & \ddots & \vdots \\ 0 & 0 & 0 & \dots & \lambda(N) \end{bmatrix} \tag{11}$$

where

$$\lambda(k) = \sum_{n=0}^{N-1} p_n e^{-2\pi ikn/N} \tag{12}$$

From this definition, it is seen that elements on the diagonal of Λ form the DFT of p. Finally, the diagonalized expression of P is introduced in the convolution product equation. In the resulting equation, the transpose operation is applied by swapping F and F^{-1} since all matrices implied are symmetrical:

$$p * g = P \cdot g = (F^{-1}\Lambda \mathrm{F})^T g = F\Lambda F^{-1} g = DFT^{-1}(DFT(p) \cdot DFT(g)) \tag{13}$$

Similar reasoning is done for the skew-circulant Q. The diagonalization brings up the Fourier matrices along with a diagonal matrix Ω [9]:

$$Q = V^{-1}\Lambda V = \Omega^{-1}\mathrm{F}\Lambda F^{-1}\Omega \tag{14}$$

with

$$\Omega = \begin{bmatrix} e^{-\frac{i\pi}{N}0} & 0 & 0 & \cdots & 0 \\ 0 & e^{-\frac{i\pi}{N}1} & 0 & & 0 \\ & \vdots & & \ddots & \vdots \\ 0 & 0 & 0 & \cdots & e^{-\frac{i\pi}{N}(N-1)} \end{bmatrix} \tag{15}$$

Similar to Eq. (12), Eq. (13) can be expressed in terms of DFT operators on vectors when considered in the skew-circulant product:

$$Q \cdot g = \Omega^{-1} F\Lambda F^{-1}\Omega g = \Omega^{-1} DFT^{-1}(DFT(p) DFT(\Omega g)) \tag{16}$$

The inverse of Ω is equivalent to its complex conjugate. Thereafter, Eqs. (14) and (16) can be summed to obtain linear convolution as presented in Eq. (6):

$$L|U \cdot g = \frac{1}{2}\left(DFT^{-1}(DFT(p) \cdot DFT(g)) \pm {\Omega_n}^{-1} DFT^{-1}(DFT(p) DFT(\Omega_n g))\right) \tag{17}$$

In time-domain NAH [3], the pressure field and the Green's function are convolved over two-dimension space and time domains, thus resulting in a three dimensional convolution:

$$\begin{aligned} p(t, x, y, z_p) &= p(t, x, y, z_0) *** g(t, x, y, d) \\ &= {\mathcal{F}_{yxt}}^{-1}\left(\mathcal{F}_{txy}(p(t, x, y, z_0))\right) \cdot G(\omega, k_x, k_y, d)) \end{aligned} \tag{18}$$

Some issues are still encountered when adapting circulant NAH to the three dimensions. At the moment, the described matrix operation is performed over the time domain for the different convolving positions in the two spatial dimensions. It would be more efficient to perform circulant matrix convolutions over the other two dimensions as well. However, since the size of the spatial domain corresponds to the number of microphones, it is usually not significant in comparison with the size of the time domain data. Thus, in terms of efficiency, the time domain is critical. Further

investigation will be achieved to fully adapt the method in 3D, possibly by performing the diagonalization of matrices of dimensions greater than two.

3. Simulation with short-time piston radiation

In this section, both standard NAH and circulant matrices based method are applied to propagate different simulated signals. The results are compared both in time and space domains to investigate the effect of wraparound. In the case of standard time-domain NAH, no zero padding has been added to the data. In circulant NAH, no padding is necessary to obtain linear convolution; in other words, the effects of the padding are present without the need to add one. In both cases, the initial signals are multiplied by a Tukey window to handle the discontinuities at the ends of the pressure field.

3.1 Effects of wraparound error in the time domain

To study the effect of zero padding in the time domain, a Gaussian pulse is simulated in MATLAB. In *x* and *y* domains, two-dimensional Gaussian function is generated over and area of 60 by 60 cm, and standard deviation of the Gaussian distribution is 10 cm. In time domain, Gaussian signal is defined over 1 ms with a standard deviation of 0.01 ms. A propagation distance of d=15 cm in the *z*-direction is applied with both NAH and circulant NAH. The results are presented in Fig. 2 at the median values in *x* and *y*.

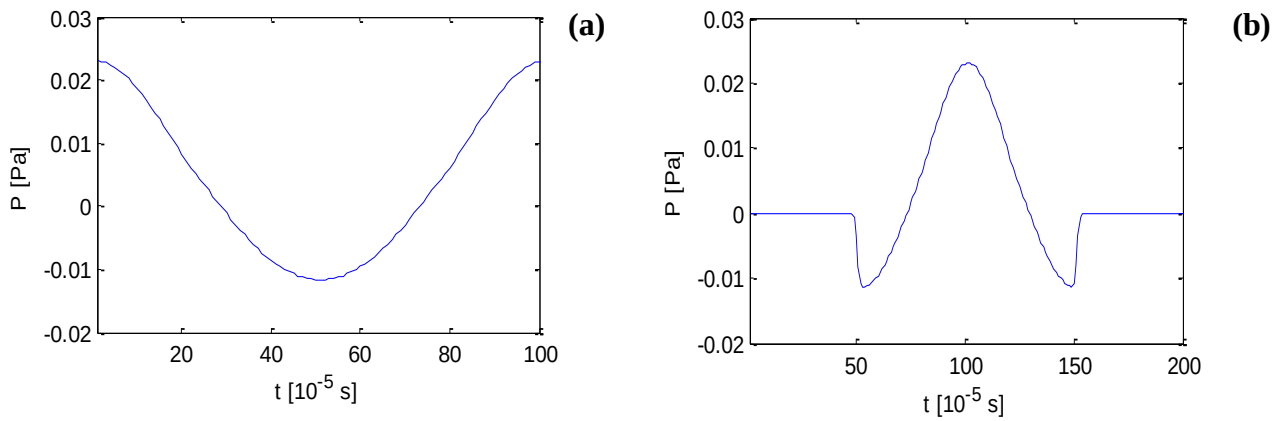

Fig 2. Propagated signals in the time domain for **(a)** standard NAH (Eq. 18) and **(b)** circulant NAH (Eq. 17)

It is noted that the resulting signal in the case of circulant NAH has twice as many values, since the convolutions are linear. For circulant NAH, values up to around 0.45 ms are null. This is expected, since it takes a certain time for the signal to reach the point of observation at c=340 m/s. Such behaviour is not observed in the case of standard NAH, which is interpreted as a causality error. Such causality errors are recurrent in the study of impact noises with NAH, and can be avoided with circulant NAH. The functions also differ significantly in amplitude as an effect of wraparound.

3.2 Effects of wraparound error in the space domain

Short-time radiation of a baffled piston is simulated in order to investigate the wraparound error in the space domain when using both standard NAH and circulant matrices based method. The sound pressure radiated by a circular piston with an arbitrary velocity profile $v(t)$ can be expressed by:

$$p(x,y,z,t) = \rho_0 h_p(x,y,z,t) \cdot \frac{d}{dt} v(t) \tag{19}$$

where h_p is the piston impulse response. [10] Coordinates x and y are in plane, and z is normal to the piston.

The piston radius used for the simulations is r_p = 4 cm. In this paper, a Gaussian velocity profile is chosen, with unitary amplitude and a width of 120 µs at half the maximum amplitude, which corresponds to a central frequency of 2800 Hz. Its velocity and acoustic pressure profiles are presented in Fig. 3. The piston sound pressure field was simulated in the plane z_0 = 5 cm with space intervals $x = y$ = 1 cm over a surface of 0.64 × 0.64 m^2. The time step was set to t = 20 µs over a duration T = 5.1 ms.

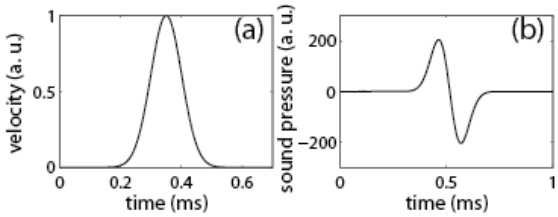

Fig 3. (a) Velocity profile of the baffled circular piston **(b)** radiated sound pressure at 5 cm along the axis

Because the data is symmetrical, values are simulated on only the first quadrant. Results in space domain are presented in Fig. 4 at fixed time t=1ms for a propagation distance of 15 cm from the source. For comparison purposes, results are presented over only the corresponding 0.64 × 0.64 m^2 area. Results are shown in two views.

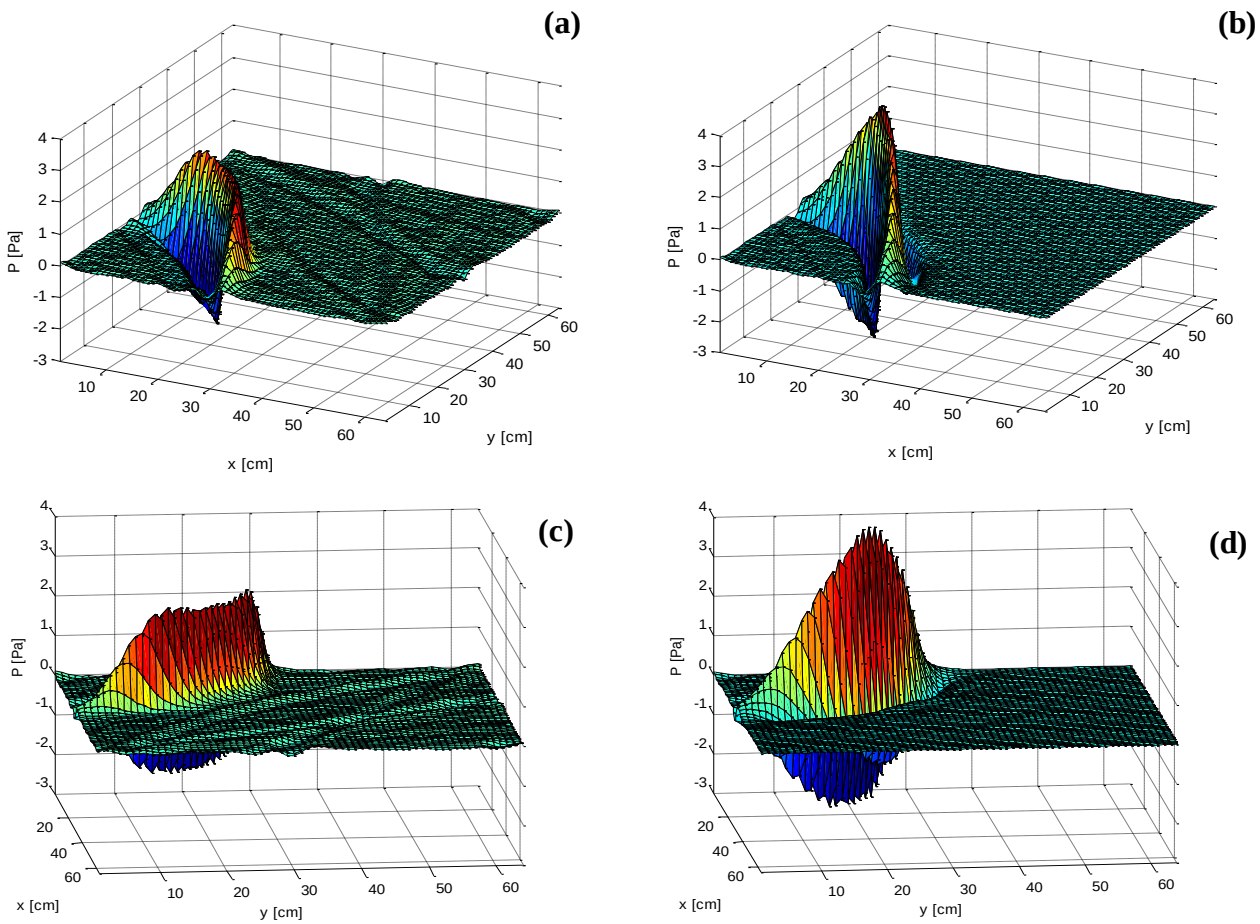

Fig 4. Propagated signals in the x and y space domain for **(a)** standard NAH (view #1), **(b)** circulant NAH (view #1) **(c)** standard NAH (view #2) and **(d)** circulant NAH (view #2)

In both cases, the wave front is predominant at r=30 cm. It is attenuated in the case of standard NAH in comparison with circulant NAH, as an effect of circular convolution. In (a) and (c), ripples are observed in the signal, both before and after the main wave front. These ripples are due to wraparound in x, y or t. In the case of circulant NAH, ripples are inexistent.

4. Conclusion

The non-periodicity of propagated transient signals is an important limitation of NAH. It was demonstrated that the use of circulant matrices based method instead of standard NAH, leads to an elimination of the wraparound error by performing a linear convolution without adding zero padding. When fully developed, this method will be computationally more efficient than standard NAH with doubled size arrays.

Preliminary results are promising. Further investigation will be done regarding the adaptation of the method to multiple dimensions.

Acknowledgments

This work was supported by the Natural Science and Engineering Research Council (Canada).

REFERENCES

[1] J. D. Maynard, E. G. Williams, Y. Lee, Near-field acoustical holography: I. Theory of generalized holography and the development of NAH. *J. Acoustical Soc. Am.* Vol **78(14)**, 1395-1413, (1985).

[2] E. G. Williams, *Fourier Acoustics, Sound Radiation and Nearfield Acoustical Holography*, Academic Press, San Diego, (1999).

[3] J. Hald, Time Domain Acoustical Holography and its Applications, J. of Sound and Vib., Vol **35**, 16-25, (2001).

[4] O. de La Rochefoucauld, M. Melon, and A. Garcia, "Time domain holography: Forward projection of simulated and measured sound pressure fields", *J. Acoust. Soc. Am*. Vol **116**, 142–153, (2004).

[5] J.-H. Thomas, V. Grulier, S. Paillasseur, J.-C. Pascal, real-time near-field acoustic holography for continuously visualizing nonstationary acoustic fields, *J. Acoustical Soc. Am.* Vol **128(6)**, 3554-3567, (2009).

[6] J.-F. Blais and A. Ross, A. Forward projection of transient sound pressure fields radiated by impacted plates using numerical Laplace transform. *J. Acoustical Soc. Am.* Vol **125(5)**, 3120-3128, (2009).

[7] P. J. Davis, *Circulant Matrices*, Chelsea Publishing, New York, NY, (1994).

[8] B. R. Hunt, A Matrix Proof of the Discrete Convolution Theorem. *IEEE Transactions on Audio and Eletronics*, Vol. **Au-19(4)**, 285-288, (1971).

[9] M. J. Narasimha, Linear Convolution Using Skew-Cyclic Convolutions, *IEEE Singal Processing Letters*, Vol **14(3)**, 137-176, (2007).

[10] P. R. Stepanishen, "Transient radiation from pistons in an infinite planar baffle", *J. Acoust. Soc. Am.* Vol **49**, 1629–1638, (1971).